INTRODUCTION

Native articular cartilage has a limited capacity for repair due to its largely avascular character. This inability to heal creates a challenge in the treatment of osteoarthritis, the degradation of articular cartilage. Osteoarthritis can be found in any joint in the body and affects over 20% of the adult population in the U.S (Helmick, 2008). One current treatment option is tissue grafting using autografts and allographs has seen limited success due to issues of tissue availability (Johma, 2002, Pallante, 2009). For years the gold standard has been total joint replacements. This highly invasive treatment is only administered for severely degenerate cases because their limited lifespan in vivo (Ravi, 2012). There is a need for a universally available treatment that is minimally invasive, able to treat osteoarthritis at earlier stages, and can maintain the function of healthy tissue in the joint.

Tissue engineering has emerged as a promising treatment solution. A host of approaches are being studied mainly centered around the in vitro culture of an autologous cell source in a 3D scaffold or pellet to attain native mechanical and biochemical properties before being implanted into injured or degenerate cartilage (Benya, 1982, Buschmann, 1992, Mauck, 2000). Engineered cartilage has been developed with similar compressive modulus and proteoglycan levels as native cartilage (Bian, 2010, Kelly, 2006, Natoli, 2009, Lima, 2007, Erickson, 2012). However, this has been achieved in small (~4 mm diameter) constructs. Larger more clinically relevant scaffolds are plagued by the inhomogeneous distribution of matrix production resulting in uneven property distributions (Bian, 2009, Buckley, 2013, Kelly, 2006). The scalability of engineered cartilage is one barrier to successful clinical translation.

The uneven distribution of properties is largely though to be a function of the diffusivity of nutrients within the scaffold and developing matrix (Nims, 2015). Matrix development on the periphery of the constructs is higher with a greater availability of nutrients and decreases toward the center (Farrell, 2012, Nims, 2014). This trend in matrix production is correlated to the compressive stiffness of the construct with higher matrix production on the periphery creating a stiffer outer shell (Khoshgoftar, 2013). As the size of the construct increases the difference in the stiffness between the periphery and center of the construct increases.

The use of macrochannels is one proposed solution to the problem of unevenly distributed mechanical properties in large tissue engineered constructs (Bian, 2009, Cigan, 2014, Nims, 2015). The addition of channels in the middle of larger constructs decreases the diffusive path and therefore increases the availability of nutrients to the middle of the constructs. Macrochannels in 10 mm constructs were shown the significantly homogenize the distribution of properties compared to solid constructs (Cigan, 2014). Similarly, dynamic loading in the bioreactor during culture was also shown to increase diffusivity and more evenly distribute properties (Kelly, 2006).

Modular tissue engineering systems have also been applied to cartilage tissue engineering to increase the size of constructs. This has been used to combine cultured rings into tube-like construct for tracheal reconstruction; to combine pellet cultures into larger sheets of engineered cartilage and to build larger sheets of scaffold based articular cartilage (Dikina, 2015, Bhumiratana, 2014, Mori, 2014). All of these modular platforms take advantage of the ability of engineered constructs' inherent stickiness and ability to form bonds. Particular to agarose models, this phenomenon of the outgrowth of cell clusters from agarose suspensions was described by Ng et al., 2012.

The Modular Engineered Tissues Surfaces (METS) technique was developed in our lab as a method to build engineered cartilage on clinically relevant scales. It utilizes the propensity of the constructs to form bonds and combine into modular scalable surfaces. Cylindrical constructs are cultured individually early in culture maximizing nutrient diffusion. They are then joined leaving macrochannels in between constructs (Figure 1). The METS technique provides a platform by which current bioreactor, biochemical, and scaffold optimization of engineered cartilage constructs can be readily scaled into clinically relevant cartilage implants. The objective of this study was to evaluate the METS technique as a solution to creating large engineered cartilage with evenly distributed properties. This was done by characterizing the spatial distribution of the biochemical and mechanical properties of METS scaffolds compared to well characterized 4 mm constructs.

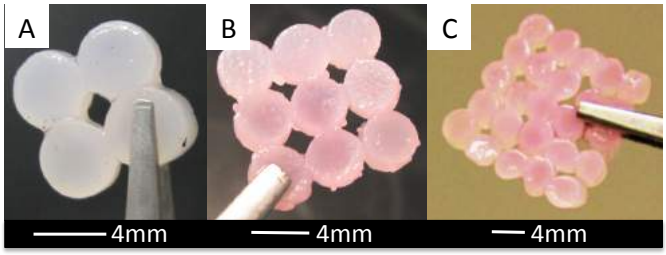

Figure 1. METS from in 2 x 2 (A), 3 x 3 (B), and 5 x 5 (C) configurations.

METHODS

This report outlines results from a series of four studies, summarized in Table 1. The first study aimed to prove the feasibility of the technique with a 2 x 2 METS. The second study aimed to repeat the results in study 1, scale up to 3 x 3 METS, manipulate the construct geometry for greater bond area, and utilize higher order passages to increase the cell yield. This study had many challenges that resulted in inconclusive results. Therefore, study three was a simplified repetition of study 2. Study 3 scaled up to 3 x 3 METS and quantified the spatial distribution of mechanical and biochemical properties of the METS. Finally, study 4 again increased the size of the METS to 5 x 5 or 400 mm^2. This represents a clinically relevant sized scaffold. The goal of this study was to determine if the spatial distribution of biochemical and mechanical properties was homogenous and compare the METS technique to the macrochannel technique already known in the literature to improve property homogeneity.

Table 1. Summary of Studies

Study	Control	METS
1		
2		Circle Octagon
3	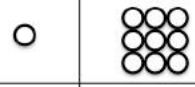	
4	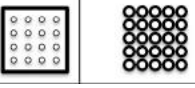	

Table 2. Approximate Study Timeline

Week	Task	Time From Last Step
1	Order Tissue	Monday
	Harvest - Passage 1	4-5 days
2	Passage 2	4 - 6 days
3	Cast	4-6 days
	Punch constructs & Day 0 testing	1 day
	Put METS in baskets	3-7 days
5	Day 14 testing	
7	Day 28 testing	
9	Day 42 testing	
10	Biochemical assays	
11	Biochemical assays	

An approximate timeline for a single study is outlined in Table 2. The tissue culture process can be divided into the following processes: chondrocyte harvesting, cell expansion, casting, culture, METS formation, mechanical testing, biochemical testing, and visual characterization. Four studies were conducted with different test groups as outlined in Table 1. The following is the generalized procedure along with a description of the variations for each study. Table 3 summarizes the testing and culture parameters that varied between the test groups.

Tissue Harvesting

Juvenile bovine knees (3-6 weeks old, n = 2-3) were purchased from Green Village butcher in New Jersey. Knees were harvested within two days of sacrifice. Cartilage was harvested per Protocol A (Appendix A). After harvest the tissue was digested with Type IV collagenase serum medium (DMEM, Invitrogen Co., Carlsbad, CA, USA) per protocols B & C and the cells were counted per the Protocol B & C.

Table 3. Summary of Variables in Each Study

	Basket 2	Basket 3			Basket 4	Basket 5
METS size	2 x 2	2 x 2	3 x 3	3 x 3	3 x 3	5 x 5
METS Shape	Circle	Circle	Circle	Octagon	Circle	Circle
Put in Baskets	Day 7	Day 7			Day 4	Day 3
Taken out of Baskets	At test	At test			Day 24	At test
Testing on Day	21, 28, 35, 42	21, 35			14, 21, 28	14, 28
Agarose	Type VII	Type IX			Type VII	Type VII
Compression Testing	All METS	Individual			Individual	Individual
Spatial variation	No	No	Yes	Yes	Yes	Yes
Controls	Single	Single			Single	Macrochannel and single
mL media/construct	1	1			1	3
Cells/mL	30 million	47 million	30 million	30 million	30 million	30 million

Cell Expansion

The chondrocytes were plated on 2-4 plates at 11 million cells per plate and expanded with 10% FBS media (Protocol E) supplemented with a growth factor cocktail (10% FBS, 1% PSAM, 1 ng/mL PDGF, 0.5 ng/mL FGF, and 0.5 ng/mL TGF) (O'Connell, 2014). Media was replaced two times per week. Cells were passaged twice to achieve sufficient cell numbers for tissue engineering studies and to improve matrix production in 3D cultures (Protocol D) (Tan, 2015). The average number of cells yielded in each passage is summarized in Table 4. The second passage used 12-20 plates depending on the required cell yield. Total cell yields for a given study were approximated using Table 5. This assumes an approximate 75% yield of testable METS from the total construct number. Cells typically became confluent in 4-6 days.

Table 4. Number of cells per plate

Total Cells (millions)					
	Harvest	P1	P2	P3	P4
Basket 3	132.2	403	1107.2	1023	1711.4
Basket 4	167.7	391.9	1152.9		
Basket 5	127.4	173.7	1618.8		
Number of Cells Trypsinized/plate (millions)					
Basket 3		N/A	92.3	N/A	N/A
Basket 4		195.9	57.6		
Basket 5		86.9	85.2		

Table 5. Construct Yield Guide

Cell Estimate Calculator			
A	Cell density (million cells/mL)	30	Constant
B	mL/gel	15	Constant
C	Constructs/gel	200	Approximate
D	Million cells/plate	100	Varies
E	**Number of plates**	**24.75**	I/D
F	**Number of constructs**	**1100**	Driver
G	Number of gels	5.5	F/C
H	mL of cells	82.5	G*B
I	Million cells	2475	A*H

Casting

Once confluence was reached the second time, passaged cells were encapsulated within agarose for a final concentration of 2% w/v agarose (Sigma-Aldrich, St. Louis, MO, USA) at a cell density of 30 x 10^6 cells/mL (Protocol F). Study two used Type IX agarose while the other studies used Type VII. Agarose was cast in the method outlined in Protocol F except for the octagonal constructs in study 2. These constructs were cast into a mold using a pipette to transfer the molten cell/agarose mixture into the mold (Figure 2). Top and bottom plates were then applied to the water jet cut acrylic mold and secured with binder clips. The octagons were then punched from the mold using a custom punch (Figure 2: inset).

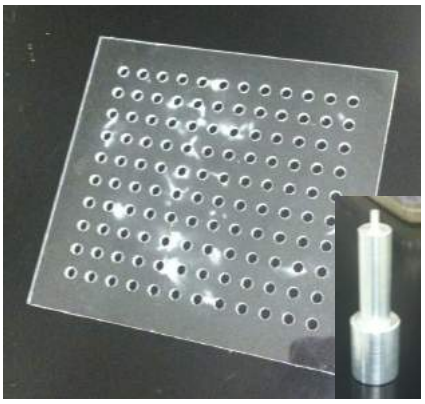

Figure 2. Octagon construct mold and punching tool.

Culture

Constructs were cultured in chondrogenic media supplemented with 10 ng/mL TGF-β3 for the first 14 days in culture (Protocol G-I). In studies one and three constructs were cultured in 1 mL/construct of media and in study four constructs were cultured in 3 mL/construct. Care was taken during feeding to minimize the movement of the constructs in the baskets and beginning in study 3

the baskets were lifted from the media following each feeding to ensure that the constructs were not flipped. Media was changed three times per week.

METS Formation

The studies compared single 4 mm diameter x 2.5 mm tall cylindrical control specimens to 2 x 2 (8 mm x 8 mm), 3 x 3 (12 mm x 12 mm), and 5 x 5 (20 mm x 20 mm) METS in studies one, two and three, and four respectively. METS were composed of constructs of equivalent dimensions to the individual controls with the exception of the octagonal construct. Study four also included a 20 mm x 20 mm square macrochannel control with 16 macrochannels of 2 mm diameter punched in approximately equivalent locations to the spaced in between METS constructs to compare the METS technique to methods that have been established in the literature to increase the spatial homogeneity of properties (Figure 3) (Cigan, 2014). To form the METS, four, nine, or twenty-five constructs were placed into a square 3D printed porous mold (Figure 4). The length and width of the molds were approximately 1 mm greater than the total construct length. In studies 1 and 2 the constructs were put into the basket at day 7 and in studies 3 and 4 the constructs were put into the baskets at day 4 and 3 respectively. For studies one, two, and four, METS remained in the baskets until testing. In study 3, METS were taken out of the baskets at day 24.

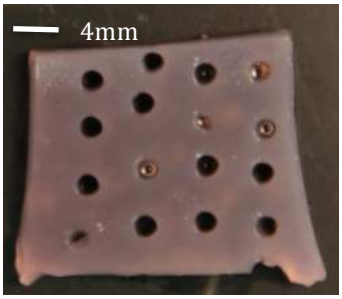

Figure 3. Macrochannel control used in study 4.

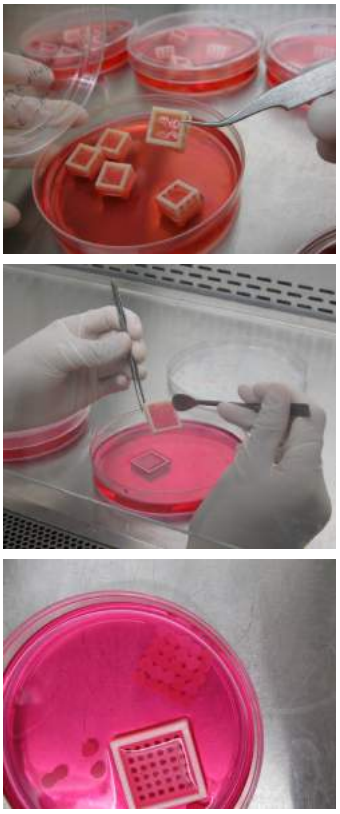

Figure 4. METS culture in study 1 (top) and study 4 (middle and bottom).

Basket development

Over the course of the studies the METS culture basket went through several iterations (Figure 5). The basket for study 1 was 9 x 9 mm accommodating 4 constructs. A previous study had used a 2 x 4 construct basket, but struggled to make repeatable bonds. To encourage full contract between the constructs the tolerances between the maximum construct dimensions and basket dimensions were reduced and a slant was added to encourage continuous contact between the constructs. This basket design was successful in forming consistent bonding between the constructs. However, the height of the basket wall made it difficult to ensure that all of the constructs were laying flat and

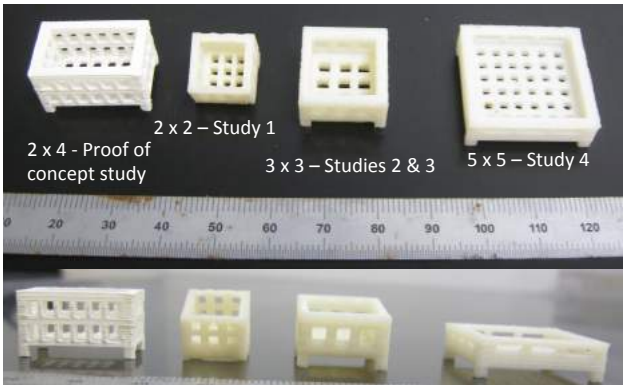

Figure 5. METS culture baskets.

resulted in many unusable METS that had a construct bonded in a side-on or flipped configuration (Figure 6). Additionally, removing the METS from the baskets was difficult and invasive due to the high walls. The METS were removed from the baskets by poking through the bottom of the basket to release any attachments to the basket.

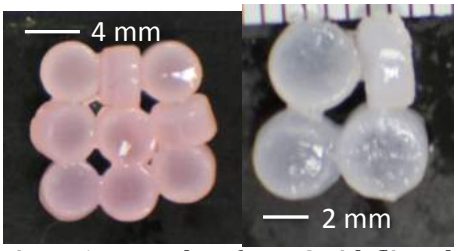

Figure 6. Examples of METS with flipped constructs.

In study 2 the baskets were scaled up to accommodate 9 constructs. The tilt was reduced because the improved connection formation was attributed to the smaller basket tolerances rather than the tilt. This was also due to the height limitations on the media depth of the dish to ensure that the baskets would be submerged. These baskets were again successful in forming bonds. However, with a higher number of constructs the probability of a construct flipping increased and there was a very low yield of flat METS (Figure 6). Although the wall height was lower than in the first study, it was still difficult to tell in the constructs were positioned correctly in a sterile environment.

The same baskets were used in study 3 as in study 2. More care was taken every time the METS were fed to ensure that none of the constructs had flipped in the first several days. Any flipped constructs were put back into place. This study still had flipped METS, but it was less than study 2.

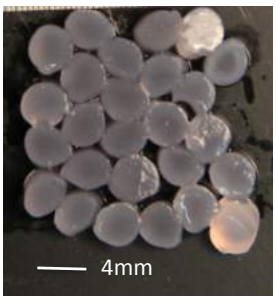

Figure 7. Larger METS had more problems with uneven macrochannel size and construct alignment.

Study 4 used baskets that were sized for 5 x 5 METS. In order to address the flipped construct issue the walls were made to be lower than the height of a construct (2 mm high for a 2.5 mm tall construct) (Figure 5). This was to make it easier to identify flipped constructs and was successful resulting in very few flipped METS. However, in this study heterogeneity in the construct dimensions reduced the accuracy of the square tessellation. The inclusion of a slightly smaller construct would allow the row to shift and collapse into the next row and reduce the size of the macrochannel spaces (Figure 7). The 5 x 5 basket could have been slightly smaller because although some disorganization may have been due to smaller constructs, there was too much space for movement when trying to create such a highly organized pattern.

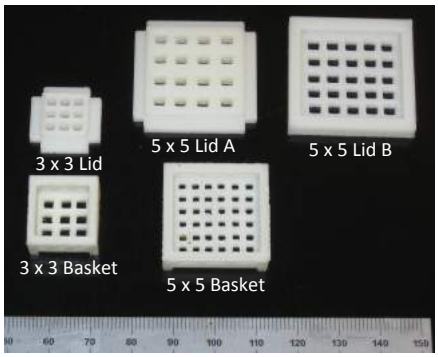

Figure 8. Lid designs that were tested to reduce construct flipping.

The use of a lid was another design that attempted to limit the ability of the constructs to flip in the baskets. Lids were designed for both the 3 x 3 and 5 x 5 baskets (Figure 8). One design was a retrofit for the existing 3 x 3 basket design. It was designed to fit within the basket and sit down into the basket depth in order to only leave 3 mm of space between the lid and bottom of the basket so that the construct would not

have room to sit up on its side. This lid was developed after the conclusion of study 3 and so was never tried. The 5 x 5 basket development began with a design that was completely a scaled up version of the 3 x 3 with tall wall and an inset lid (Figure 8 – 5 x 5 Lid A). An alternative design was the short walls with an overlaying lid that would physically keep the constructs flat (Figure 8 – 5 x 5 Lid B). This design was tested concurrently with study 3. The lid in the first design (A) floated off. The second design (B) was effective in keeping the constructs flat, but was difficult to remove without compromising the sterility of the dish. Additionally, when the lid was removed it was clear that the sandwiching of the constructs between the lid and bottom caused bonding between the constructs and both the lid and bottom and tore some of the bonds of the METS as it was lifted. From these results it was decided to eliminate the lids and rely on the short walled 5 x 5 baskets.

Mechanical Testing

Compressive mechanical properties (i.e. equilibrium and dynamic moduli) were determined at day zero to test the baseline strength of the agarose scaffold and then weekly or biweekly depending on the study (Table 3) (n = 4-5 per group per time point) to characterize the matrix production of the cells. The equilibrium modulus was measured in unconfined compression at 10% strain, and the dynamic modulus was determined from sinusoidal ± 1% strain at 0.5 Hz (Protocol J). MATLAB was used to determine the moduli using 'Instron SRL'. InstronSRL computes the equilibrium modulus as the modulus based on the last 50 data points in the relaxation curve. The dynamic modulus is calculated as the modulus of the difference between the minimum and maximum load and displacements in the dynamic loading. In study one compression testing was preformed on the connected METS sample (2 x 2) and the resultant values were divided by four to compare with individual control values. In studies two through four the METS samples were cut apart and single constructs were isolated to determine local properties.

In study one, following bulk compressive testing, each group of four was cut in half to isolate a single bond. The tensile strength of the bond was assessed using a tensile strain rate of 1 mm/min until failure. The bond length was measured optically and used to calculate the stiffness as the slope of the force normalized by area to displacement curve. The peak force at failure was also recorded. In study three, the tensile strength of the bond was assessed using a strain rate of 1 mm/s until failure of any bonds in a string of 4-5 connected constructs. Peak force at failure was recorded.

Biochemical Analysis

After mechanical testing, the wet weight was recorded. After completion of the study, all samples were lyophilized and the dry weight was recorded. The samples were digested overnight using Proteinase K and centrifuged for biochemical evaluation. Biochemical characterizations measured the levels of DNA, GAG and collagen in the samples at day 28 (Protocol K). DNA was measured using a PicoGreen (Invitrogen, Co.) assay kit. GAG was measured using a DMMB assay (Farndale, 1986) (Figure 9) and collagen (Stegemann, 1967) was measured using a hydroxyproline (OHP) assay (Figure 10).

Figure 9. GAG Assay reading.

The protocol for the OHP collagen assay was producing unreliable data. The Biotek reader was not returning equivalent values for the blank wells in the standard rows (Table 6 - A1, A2, B1, B2) and any samples wells left blank (Table 6 - Row H). Initially the sample wells were linearly corrected back to subtract this difference. However this resulted in negative readings in many samples. The assay was rerun multiple times to ensure that this was not due to an error in the assay preparation. A single plate was then run multiple times with different iterations of the protocol removing progressively more calculations by the software. A correct plate reading was achieved by removing all references to the standard curves and blank wells in the protocol. The differences were indeed non-linear which confirms the inability to subtract off the difference. While this is being resolved, all OHP data are presented as relative comparisons between groups with no confirmed values associated. In future studies the OHP protocol should be adjusted, but care should be taken to ensure that assay readings make sense.

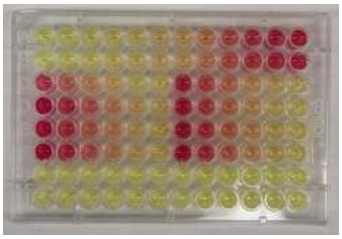

Figure 10. OHP Assay Plate.

Table 6. Example of incorrect OHP assay output.

	1	2	3	4	5	6	7	8	9	10	11	12
A	0.057	0.058	0.077	0.092	0.109	0.121	0.139	0.208	0.341	0.468	0.599	0.722
B	0.058	0.058	0.072	0.091	0.106	0.123	0.143	0.217	0.353	0.487	0.617	0.753
C	0.231	0.178	0.15	0.171	0.145	0.13	0.235	0.169	0.133	0.201	0.152	0.128
D	0.276	0.198	0.161	0.26	0.195	0.166	0.174	0.16	0.155	0.268	0.211	0.185
E	0.232	0.201	0.182	0.305	0.237	0.197	0.269	0.219	0.185	0.246	0.196	0.176
F	0.303	0.239	0.203	0.329	0.25	0.213	0.263	0.221	0.198	0.246	0.21	0.194
G	0.31	0.25	0.215	0.374	0.279	0.226	0.208	0.194	0.185	0.227	0.202	0.188
H	0.183	0.186	0.182	0.185	0.186	0.185	0.187	0.188	0.186	0.184	0.185	0.182

Visual Characterization

In study 1, 2, and 4 cell viability and distribution was evaluated using a LIVE/DEAD assay (Invitrogen Co.) and the confocal microscope available in the QB3C facility. Images were taken of the bond to characterize cell infiltration into the bond. Specimens were sectioned transversely to obtain more planar sections of the bond and to reduce the artifacts of dead cells on the surfaces resulting from handling. Single images were taken in addition to z-stacks and ATLAS surveys. Before mechanical testing the METS were viewed at 10x with a brightfield microscope. Cell patterns and structures were observed at the bond junctions. METS from study 3 (3 x 3) were fixed on day 21 in a fixative solution (3.7% formalin, 5% glacial acetic acid, 70% ethanol, and 15% distilled water) (Protocol L) [Lin, 1997]. After fixation they were stored in 70% ethanol and sent to Professor Tamara Alliston's lab at UCSF for histological analysis. The constructs and METS were infiltrated with 15% sucrose overnight, carefully blotted dry and embedded in OCT in metal embedding molds. The molds were frozen in a dry ice/isopropyl alcohol bath, and stored at -20 until sectioned. Sections were cut at 10 to 20 microns, mounted on gelatin subbed slides, and dried at room temp overnight. Slides were stored at -20 until stained. Immunohistochemical staining for aggrecan was done using antibody 12/21/1-C-6-c from the Developmental Studies Hybrioma Bank. A

Vectastain ABC kit (Vector, cat# PK4000) was used with a primary antibody dilution of 1:100 for 1 hour at room temperature.

Statistical Analysis

A one-way ANOVA with Tukey post hoc HSD analysis was used to compare changes in mechanical and biochemical properties by location and over time. A Student's t-test was used to compare tensile properties between time points. Significance was set at $p \leq 0.05$. Data are presented as mean ± standard deviation.

RESULTS

During culture constructs were observed to begin to stick together in culture at day 3. For this reason in the third and forth studies the METS were put into the baskets earlier than day 7. By day 14, stable connections had formed between constructs in METS samples.

Several macroscopic observations were made of the construct shape and composition. An observable change in opacity and bond size occurred throughout the culture period. Constructs started out as slightly translucent and became progressively more opaque over the culture period. Figure 12 shows white edges and a dark middle of the construct characteristic of the first few weeks of culture. Similarly, on day 14, the bonds were weak and care was taken during any handling, but by day 21 onwards the bonds were robust and the METS could be manually handled with little worry of breaking the bonds. In studies 2 and 3 many protrusions were observed on the edges of the constructs (Figure 12). Specific to the octagonal constructs these protrusions were attributed to damage during removal from the mold that resulted in imperfect shapes and protrusions (Figure 12). However, this was also observed in some of the round constructs. It was likely due to matrix production and over confluence during expansion that was not filtered out. During punching this matrix led to rough edges and excess material attached to the constructs, which then developed into 'arms'. This could be avoided by filtering the cells prior to casting, using a sharp biopsy punch for each gel, and taking care to create even punches.

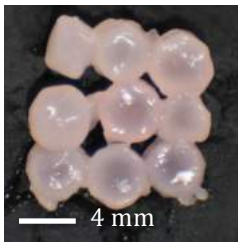

Figure 12. Example of octagonal METS in study 2 with uneven coloration and protrusions.

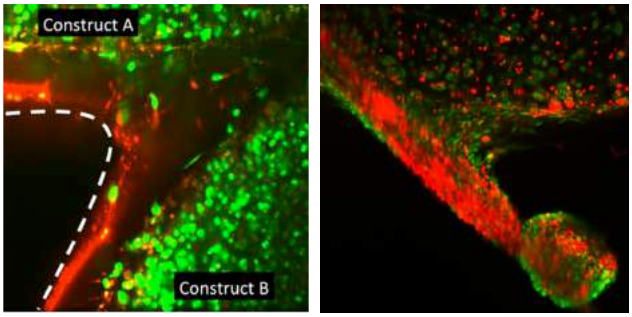

Figure 13. Confocal imaging in study 2 (left) showing live cell infiltration (green) into METS junction and cell protrusion from study 4 (left) with appreciable cell death (red).

Confocal images showed infiltration of elongated living cells in the junctions (Figure 13) and cell aggregations on the periphery of the construct. Confocal imaging also revealed an appreciable level of cell death in both the first and fourth studies (Figure14). Cellular infiltration of the connections was further characterized through histology (Figure 15) showing clear new tissue formation in the junction. Cell aggregations in ball-like protrusions were commonly observed with bright field microscopy in METS junctions and

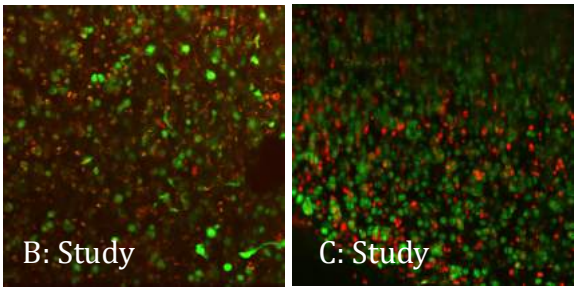

Figure 14. Comparison of live (green) and dead (red) cell

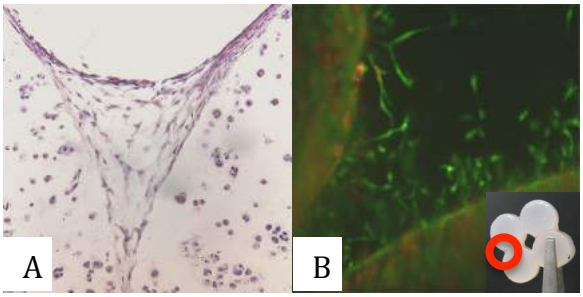

Figure 15. Cell infiltration into METS junction imaged using histology (A) and confocal microscopy (B).

at the construct periphery (Figure 17 A-C). Tissue deposition in the bonds was also observed optically with fibrous structures connecting constructs (Figure 17 D-F). No trends in the structure of the cell formations were observed over time.

Channels (approximately 2mm in diameter) formed between constructs remained open throughout the culture period. In study one, day 28, the bond width was 2.2 ± 0.3 mm and the tensile mechanical properties of the bonds increased over time (day 21 versus day 28, $p < 0.05$, Figure 18). In study four, peak bond force similarly increased from 0.15 ± 0.16 N on day 14 to 0.6 ± 0.13 N on day 28 ($p = 0.02$, data not shown).

Compressive mechanical properties of METS and individual constructs increased over time. In study one, at day 28, constructs were 3-9 times greater than initial properties ($p < 0.01$, Figure 19). Similarly in studies three and four compressive mechanical properties were at least 2.7 times greater than initial properties ($p < 0.03$, data not shown). At day 28, there were no significant differences in dynamic and equilibrium moduli between individual

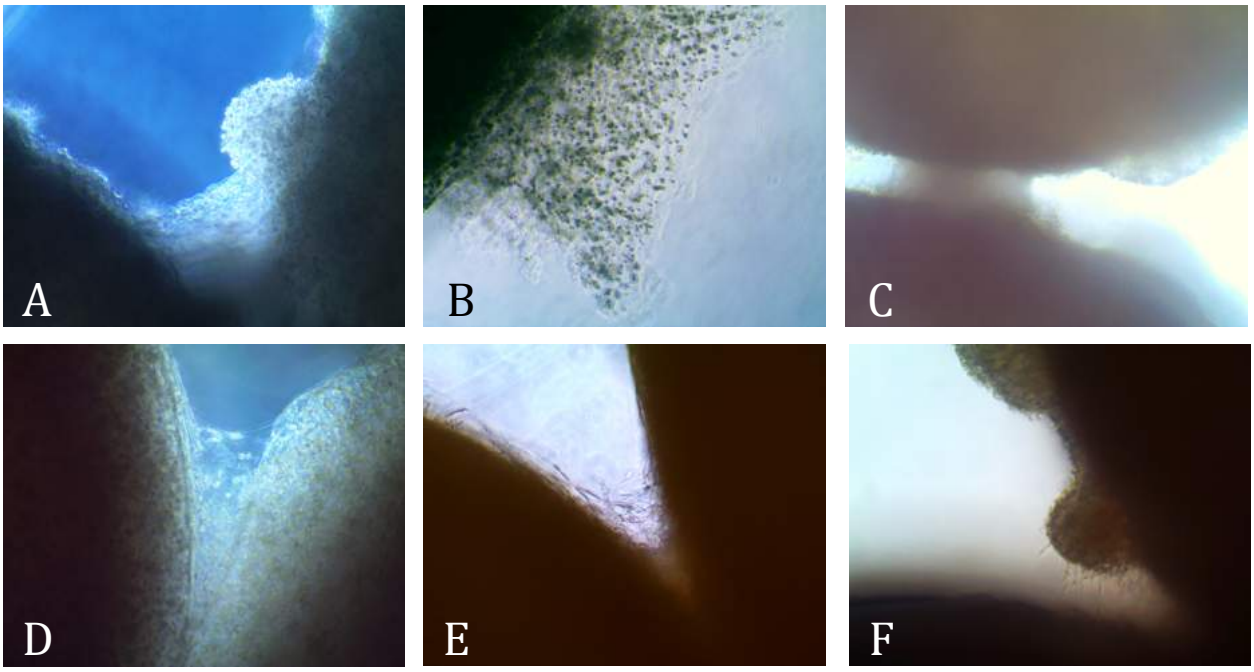

Figure 17. Observations in the METS junctions viewed at 10x with a Brightfield microscope. Cell aggregates seen in studies 3, 1, and 3 (A, B, and C respectively) and fibrous structures between constructs in study 4 (D) and study 1 (E) and emanating from cell aggregates near the METS junction in study 1 (F).

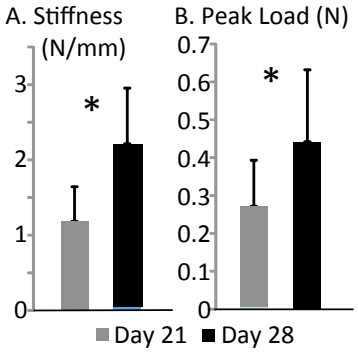

Figure 18. Tensile stiffness (A) and peak load (B) at failure of the METS bond (Study 1) increased over time (p<0.05).

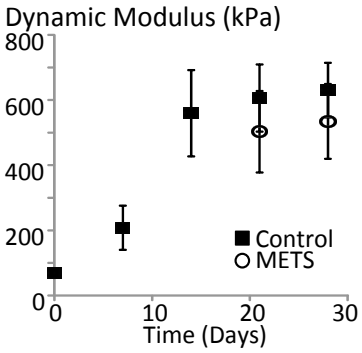

Figure 19. The compressive dynamic modulus of the METS and individual controls (Study one) increased over time.

constructs and METS samples for all studies (p > 0.07).

There was no difference observed in the spatial distribution of equilibrium or dynamic modulus in 3 x 3 or 5 x 5 METS compared to an individual control (study 2: p > 0.07; study 3: p > 0.18). The 3 x 3 METS demonstrated an expected trend with the highest equilibrium modulus 47.2 kPa ± 15.5 kPa in the corner followed by 42.9 kPa ± 23.1 kPa on the side and 35.3 kPa ± 18.0 kPa in the center compared to the single control at 61.174 kPa ± 11.7 kPa (Figure 20). This trend was mirrored by the dynamic moduli, but was not statistically significant. The pattern was not repeated in study four. In study four the equilibrium moduli were 37.0 kPa ± 26.3 kPa, 58.0 kPa ± 34.7 kPa, 66.1 kPa ± 26.4 kPa, and 32.4 kPa ± 13.3 kPa for the control, corner, middle, and center of the METS respectively.

In study four the METS technique was compared to large constructs with macrochannels. The macrochannel controls showed a similar trend as the METS samples with statistically similar equilibrium and dynamic compressive moduli to individual controls (p > 0.38). However, compressive equilibrium modulus of the macrochannel controls were nominally lower than the METS (p < 0.07) with a significantly lower in dynamic modulus 152.3 kPa ± 49.7 kPa for the macrochannel controls compared to 296.2 kPa ± 133.6 kPa for the METS (p = 0.01) (Figure 21).

Biochemical assays demonstrated that METS were similar to or had higher DNA, GAG, and collagen contents compared to individual controls (p > 0.05 unless otherwise stated, Figure 20 & 22). In cases where the DNA, GAG, or collagen content was higher in the METS, this finding was never repeatable in another study. In study one the GAG content of METS samples was 29% greater than the control (p < 0.01, data not shown). In study four the DNA content of the center of the METS was significantly greater than the single control and corner METS (p = 0.04, Figure 22). The GAG content in study four was significantly different between the METS outer constructs and the mid-section macrochannel control (p = 0.005, Figure 22). No trends in spatial distribution of biochemical properties were observed to be

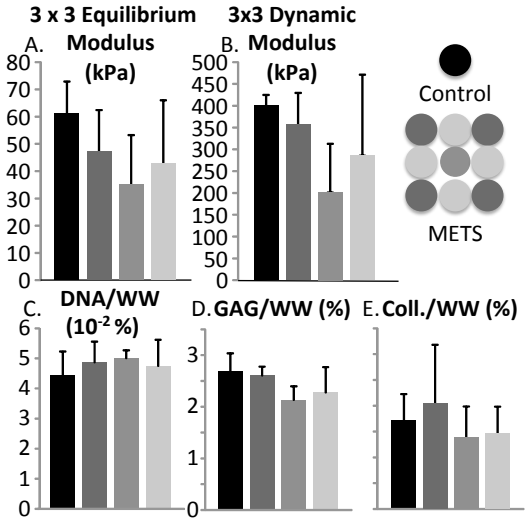

Figure 20. Spatial distribution of the equilibrium (A) and dynamic (B) compressive modulus and biochemical properties, DNA (C), GAG (D), and collagen (E) composition of individual controls and 3 x 3 METS

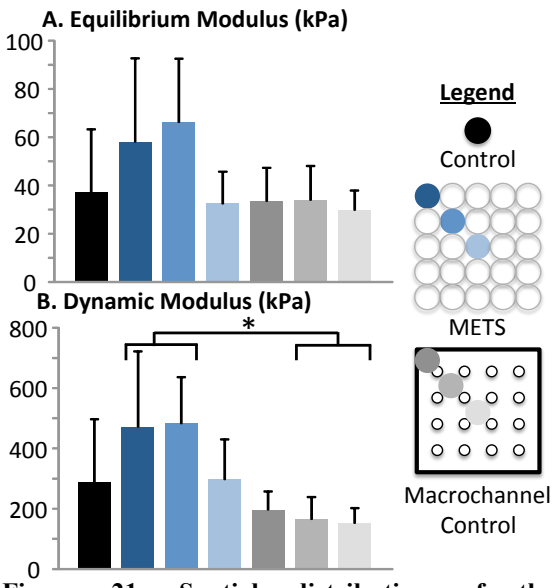

Figure 21. Spatial distribution of the equilibrium (A) and dynamic (B) compressive modulus of individual, METS, and macrochannel controls in study three.

repeatable between studies.

DISCUSSION

This study demonstrates that the METS technique is a viable method for forming large (400 mm^2) tissue engineered cartilage surfaces. The METS had similar or improved biochemical and mechanical properties when compared to individual 4 mm diameter controls. Throughout the culture period the macrochannel spaces between joined constructs remained open allowing continuous nutrient supply. Previous macrochannel studies have shown the occlusion of macrochannels (Cigan, 2014, Nims, 2015). We attribute the size of the METS macrochannels (~ 2 mm diameter compared to 1 mm (Cigan, 2014)) to maintaining open macrochannels throughout the 35-day culture period. This may prove efficacious during implantation.

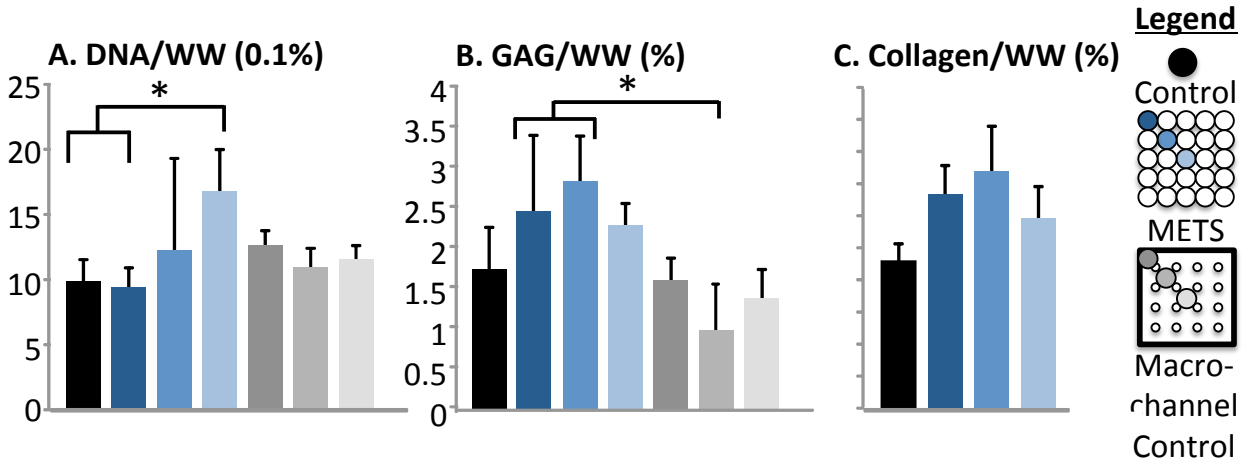

Figure 3. DNA (A), GAG (B), and collagen (C) content of individual controls, METS, and macrochannel controls in study three. DNA content was significantly higher in the METS than the individual control (p=0.04). GAG content was significantly higher in METS than macrochannel controls (p=0.006). Collagen content was significantly higher in the METS than the individual controls (p=0.008) and macrochannel controls ($p<10^{-11}$).

Macrochannels can provide locations for native cells to infiltrate and affix the implant. The METS technique holds good clinical potential as a tissue-engineering analogue to mosaicplasty repair by which a surgeon grafts smaller circular punches of cartilage into a large defect (Hangody, 2003).

The bonds that formed between constructs were shown to increase in strength over time and were within the range of values reported for the tensile strength of bovine articular cartilage (Danso, 2014). Cell infiltration into the bond was observed suggesting that cell

migration was occurring in response to the proximity of neighboring constructs. These finding are similar to those outlined in other work that exploits the self-assembly binding of tissue engineered constructs (Bhumiratana, 2014, Dikina, 2015, Mori, 2014).

The METS had bulk compressive equilibrium and dynamic moduli statistically similar to a single 4 mm diameter construct. The METS technique also did not have statistically lower biochemical properties to the individual control. In study four, the DNA and, in study one, GAG level in the METS were significantly higher than individual controls. However, since this trend was not repeatable between studies it is not being considered significant.

The METS technique created scaffolds with evenly distributed mechanical and biochemical properties. This is similar to previous results using macrochannels punched into bulk constructs on day zero. Comparing the METS to macrochannel controls, the equilibrium modulus of the macrochannel controls was nominally lower that that of the METS and the dynamic modulus of the inner macrochannel controls was significantly lower than the outer METS. This suggests that there is a benefit in initially culturing constructs individually to maximize nutrient availability before creating large surfaces.

This technique builds on established tissue engineering accomplishments of developing constructs with similar properties to native cartilage. The compressive mechanical and biochemical properties reported in this study remain below that of native tissue. However, the METS technique presented here can be extrapolated broadly in the field to produce large engineered surfaces from many small-scale ($\sim$ 15 mm^2) efforts. Thus, the METS technique can be applied to the state of the art advancements that have been achieved in cartilage tissue engineering to build larger, clinically scaled surfaces.

Several challenges extended through each of these studies. Studies 1, 2, and 3 suffered from poor yields due to flipped constructs. Study 4 had high geometric heterogeneity of the constructs. This was due to imperfect circles following punching and punching circles from the macrochannel controls with uneven distribution of channels. This was likely the cause for the much higher standard deviations in study 4. Additionally, agarose protrusions or cell aggregations on the edges or faces of the constructs led to uneven distribution of load during compressive testing. In future studies extreme care should be taken to control the shape and size of the mechanical test specimens.

Future work will focus on combining the METS technique with known methods to further increase nutrient transport and compressive stiffness such as the use of a bioreactor for dynamic loading and perfusion (Cigan, 2014, Chabine, 2009, Bian, 2010). Preliminary work has been done to demonstrate the feasibility of using the bioreactor in the O'Connell lab to work in a sterile environment for organ culture. However, translation for working with cell culture will require significant modification to the system for repeatable and sterile loading of METS constructs in their culture baskets. Initial work has also been done to demonstrate the feasibility of creating METS in patient specific 3-D contours by creating molds from CT scans. A METS basket was developed from a CT scan of a tibial plateau (Figure 23) with porous walls, but a solid bottom. It has not been used in a study. The full basket would hold approximately 100 constructs and pose new challenges in construct alignment. Potential

solutions to these challenges would be to create square or cylindrical constructs with equal height and diameter to eliminate the need for all constructs to lay flat. Different sized constructs may also be required to accommodate the irregular shape.

Figure 23. CT of tibial plateau converted to a solid model for modification into a basket surface.

This study was limited by a low sample size (n=4-5). Although the ANOVA analysis showed significance of many results, there is likely not enough statistical power to overcome the high standard deviations. Given these limitations this work attempts to characterize the METS technique. Future studies will expand the sample sizes to yield stronger results.

In conclusion, the METS technique presents a method for creating engineered cartilage surfaces on clinically relevant scales with evenly distributed biochemical and mechanical properties. It utilizes the propensity of agarose constructs to stick together in culture along with the presence of macrochannels to supply nutrients throughout the surface. This leads to a robust method for developing modular surfaces that can be scaled and shaped to patient specific geometries. The METS technique provides a process to overcome the size limitations on engineered cartilage.

AKNOWLEDGEMENTS

I would like to acknowledge and thank the following people for their contribution to this work: Dr. Grace O'Connell for advising the training, Dr. Tamara Alliston and Ellen Liebenberg for histological staining and imaging, Wan Fung Chui, Anne Zeng, Joao Innocente de Souza, Aditya Nandy, Gerald Santos, Leslie Girard, and Jackson Hendershott for assistance during culture and testing, and Mary West with her assistance with confocal imaging. I would also like to thank our funding sources: The Rose Hills Innovator Award, UC Berkeley, and the Student Mentoring and Research Teams (SMART) Program, UC Berkeley.

REFERENCES

1. Helmick, Charles G., Felson, David T., Lawrence, Reva C., Gabriel, Sherine, Hirsch, Rosemarie, Kwoh, C. Kent, Liang, Matthew H., Kremers, Hilal Maradit, Mayes, Maureen D., Merkel, Peter A., Pillemer, Stanley R., Reveille, John D., Stone, John H., Estimates of the Prevalence of Arthritis and Other Rheumatic Conditions in the United States, Arthritis and Rheumatism, (2008) 58:1:15-25.

2. Jomha, N.M., Lavoie, G., Muldrew, K., Schachar, N.S., McGann, L.E., Cryopreservation of intact human articular cartilage, Journal of Orthopaedic Research (2002) 20: 1253-1255

3. Pallante, Andrea L., et al. "Chondrocyte viability is higher after prolonged storage at 37 C than at 4 C for osteochondral grafts." *The American journal of sports medicine* 37.1 suppl (2009): 24S-32S.

4. Ravi, Bheeshma, et al. "The changing demographics of total joint arthroplasty recipients in the United States and Ontario from 2001 to 2007." *Best practice & research Clinical rheumatology* 26.5 (2012): 637-647.

5. Benya, Paul D., Shaffer, Joy D., Dedifferentiated Chondrocytes Reexpress the Differentiated Collagen Phenotype When Cultured in Agarose Gels, Cell (1982) 30:215-224.

6. Buschmann, Michael D., Gluzband, Yehezkiel A., Grodzinsky, Alan J., Kimura, James H., Hunziker, Ernst B., Chondrocytes in Agarose Culture Synthesize a Mechanicaly Functional Extracellular Matrix, Journal of Orthopaedic Research, (1992) 10:745-758.

7. Mauck Robert L., Soltz Michael A., Wang Christopher C. B., et al. Functional Tissue Engineering of Articular Cartilage Through Dynamic Loading of Chondrocyte-Seeded Agarose Gels J Biomech Eng 122(3), 252-260 (2000) (9 pages); doi:10.1115/1.429656

8. Erickson, I. E., Kestle, S. R., Zellars, K. H., Farrell, M. J., Kim, M., Burdick, J. A., & Mauck, R. L. (2012). High mesenchymal stem cell seeding densities in hyaluronic acid hydrogels produce engineered cartilage with native tissue properties. Acta biomaterialia, 8(8), 3027-3034.

9. Bian, Liming, Fong, Jason V., Lima, Eric G., Stoker, Aaron M., Ateshian, Gerard A., Cook, James L., Hung, Clark T., Dynamic Mechanical Loading Enhances Functional Properties of Tissue-Enigineered Cartilage Using Mature Canine Chondrocytes, Tissue Engineering Part A (2010) 16:5, 1781-1790.

10. Kelly, Terri-Ann N., et al. "Spatial and temporal development of chondrocyte-seeded agarose constructs in free-swelling and dynamically loaded cultures."*Journal of biomechanics* 39.8 (2006): 1489-1497.

11. Natoli, Roman M., Response, Donald J., Lu, Benjamin Y., Athanasiou, Kyriacos A., Effects of Multiple Chondroitinase ABC Applications on Tissue Engineered Articular Cartilage, Journal of Orthopaedic Research, (2009) 27:7:949-956.

12. Lima, E.G., Bian, L., Ng, K.W., Mauck, R.L., Byers, B.A., Tuan, R.S., Ateshian, G.A., Hung, C.T., The beneficial effect of delayed compressive loading on tissue-engineered cartilage constructs cultured with TGF-B3, Osteoarthritis and Cartilage (2007) 15:1025-1033.

13. Nims, Robert J., et al. "Matrix production in large engineered cartilage constructs is enhanced by nutrient channels and excess media supply." *Tissue Engineering Part C: Methods* (2015).

14. Bian, L., Angione, S.L., Ng, K.W., Lima, E.G., Williams, D.Y., Mao, D.Q., Ateshian, G.A., Hung, C.T., Influence of decreasing nutrient path length on the development of engineered cartilage, Osteoarthritis and Cartilage (2009) 17, 677-685

15. Buckley, Conor T., Meyer, Eric G., Kelly, Daniel J., The Influence of Construct Scale on the Composition and Functional Properties of Cartilaginous Tissues Engineered Using Bone Marrow-Derived Mesenchymal Stem Cells, Tissue Engineering Part A (2013) 18:3&4:362-396.

16. Farrell, Megan J., Comeau, Eric S., Mauk, Robert L., Mesenchymal stem cells produce functional cartilage matrix in three-dimensional culture in regions of optimal nutrient supply, European Cells and Materials (2012) 23:425-440.

17. Nims, Robert J., et al. "Synthesis rates and binding kinetics of matrix products in engineered cartilage constructs using chondrocyte-seeded agarose gels."*Journal of biomechanics* 47.9 (2014): 2165-2172.

18. Khoshgoftar, Mehdi, et al. "Influence of the temporal deposition of extracellular matrix on the mechanical properties of tissue-engineered cartilage." *Tissue Engineering Part A* 20.9-10 (2014): 1476-1485.

19. Cigan, Alexander D., Nims, Robert J., Albro, Michael B., Vunjak-Novakovic, Gordana, Hung, Clark T., Ateshian, Gerard A., Nutrient channels and stirring enhanced the composition and stiffness of large cartilage constructs, Journal of Biomechanics (2014) 47:3847-3854.

20. Dikina, Anna D., et al. "Engineered cartilaginous tubes for tracheal tissue replacement via self-assembly and fusion of human mesenchymal stem cell constructs." *Biomaterials* 52 (2015): 452-462.

21. Bhumiratana, Sarindr, et al. "Large, stratified, and mechanically functional human cartilage grown in vitro by mesenchymal condensation." *Proceedings of the National Academy of Sciences* 111.19 (2014): 6940-6945.

22. Mori, Yoshiyuki, Kanazawa, Sanshiro, Asawa, Yukiyo, Sakamoto, Tomoaki,Inaki, Ryoko, Okubo, Kazumi, Nagata, Satoru, Komura, Makoto, Takato, Tsuyoshi, Hoshi, Kazuto, Regenerative Cartilage made by Fusion of Cartilage Elements derived from Chondrocyte Sheets prepared in Temperature-Responsive Culture Dishes, Journal of Hard Tissue Biology (2014) 23[1]:101-110.

23. Ng, Soon Seng, Su, Kai, Li, Chuan, Chan-Park, Mary B., Wang, Dong-An, Chan, Vincent, Biomechanical study of the edge outgrowth phenomenon of encapsulated chondrocytic isogenous groups in the surface layer of hydrogel scaffolds for cartilage tissue engineering, Acta Biomaterialia, (2012) 8:244-252.

24. O'Connell, G. D., et al. "Time and dose-dependent effects of chondroitinase ABC on growth of engineered cartilage." *European cells & materials* 27 (2014): 312.

25. Tan, Andrea R., et al. "Passage-dependent relationship between mesenchymal stem cell mobilization and chondrogenic potential." *Osteoarthritis and Cartilage*23.2 (2015): 319-327.

26. Farndale, Richard W., David J. Buttle, and Alan J. Barrett. "Improved quantitation and discrimination of sulphated glycosaminoglycans by use of dimethylmethylene blue." *Biochimica et Biophysica Acta (BBA)-General Subjects* 883.2 (1986): 173-177.

27. Stegemann, Hermann, and Karlheinz Stalder. "Determination of hydroxyproline." *Clinica Chimica Acta* 18.2 (1967): 267-273.

28. Lin W, Shuster S, Maibach HI, Stern R. Patterns of hyaluronan staining are modified by fixation techniques. *J Histochem Cytochem.* 1997 Aug;45(8):1157-63.

29. Danso, E. K., et al. "Comparison of nonlinear mechanical properties of bovine articular cartilage and meniscus." *Journal of biomechanics* 47.1 (2014): 200-206.

30. Chahine, Nadeen O., Albro, Michael B., Lima, Eric G., Wei, Victoria I., Dubois, Christopher R., Hung, Clark T., Ateshian, Gerard A., Effect of Dynamic Loading on the Transport of Solutes into Agarose Hydrogels, Biophysical Journal (2009) 97, 968-975.

31. Hangody, László, and Péter Füles. "Autologous osteochondral mosaicplasty for the treatment of full-thickness defects of weight-bearing joints." *The Journal of Bone & Joint Surgery* 85.suppl 2 (2003): 25-32.

32. O'Connell, Grace D., et al. "Toward engineering a biological joint replacement."*The journal of knee surgery* 25.3 (2012): 187.

Appendix A: Protocols

Protocol A: Harvesting Bovine Knee Chondrocytes
Protocol B: Tissue Digestion Protocol
Protocol C: 5% FBS Media Protocol
Protocol D: Cell Passaging and Counting Protocol
Protocol E: 10% FBS Media Protocol
Protocol F: Casting Protocol
Protocol G: Chondrogenic Media Protocol
Protocol H: DMEM Protocol
Protocol I: Construct Feeding Protocol
Protocol J: SRL Compression Testing Protocol
Protocol K: Biochemical Assay Protocol
Protocol J: Histology Protocol